Spin diode behavior in transport through single-molecule magnets

M. Misiorny[1], I. Weymann[1,2] and J. Barnaś[1,3]

[1] *Faculty of Physics, Adam Mickiewicz University, 61-614 Poznań, Poland*
[2] *Physics Department, Arnold Sommerfeld Center for Theoretical Physics and Center for NanoScience, Ludwig-Maximilians-Universität München, 80333 München, Germany*
[3] *Institute of Molecular Physics, Polish Academy of Sciences, 60-179 Poznań, Poland*

PACS 85.75.-d – Magnetoelectronics; spintronics: devices exploiting spin polarized transport or integrated magnetic fields
PACS 75.50.Xx – Magnetic devices: molecular magnets
PACS 72.25.-b – Spin polarized transport

Abstract. - We study transport properties of a single-molecule magnet (SMM) weakly coupled to one nonmagnetic and one ferromagnetic lead. Using the diagrammatic technique in real time, we calculate transport in the sequential and cotunneling regimes for both ferromagnetic and antiferromagnetic exchange coupling between the molecule's LUMO level and the core spin. We show that the current flowing through the system is asymmetric with respect to the bias reversal, being strongly suppressed for particular bias polarizations. Thus, the considered system presents a prototype of a SMM spin diode. In addition, we also show that the functionality of such a device can be tuned by changing the position of the molecule's LUMO level and strongly depends on the type of exchange interaction.

Introduction. – Due to their particular physical properties, such as an energy barrier for the spin reversal or long relaxation times [1], single-molecule magnets (SMMs) are inherently predestined for applications in novel molecular electronic or spintronic circuits [2, 3]. Up to now, several different physical mechanisms employing SMMs as a key component have been theoretically considered. It has been in particular shown that the SMM's spin can be reversed by means of spin polarized currents [4–6], or by applying a spin bias [7]. Furthermore, when bridged between two nonmagnetic metallic leads a SMM can work as a spin filter [8, 9]. Recent experiments on electronic transport through SMMs connected to metallic but nonmagnetic leads [10–14] clearly show that the aforementioned ideas are in principle experimentally feasible. From a conceptual point of view, the simplest realization of a system consisting of a SMM attached to one ferromagnetic and one nonmagnetic reservoir could be a device involving the scanning tunneling microscope (STM) with a magnetic tip and a SMM on a metallic but nonmagnetic substrate, Fig. 1(a). The advantage of such a geometry is that by choosing an appropriate ligand shell for the molecule, one can obtain the specific orientation (e.g. parallel) of the molecule's easy axis with respect to the surface [15]. Furthermore, there are experimental techniques which allow for deposition of a film of well-dispersed SMMs on a substrate, enabling access to individual molecules with the STM tip [16–20]. Thus, it is interesting to consider how transport properties of a SMM change if one of two metallic nonmagnetic leads is replaced by a magnetic one.

In this Letter we study in general transport through a SMM weakly coupled to electrodes with unequal spin polarizations. As already shown in the case of quantum dots [21–24], transport properties of such systems exhibit a significant asymmetry with respect to the bias reversal. In addition, due to coupling to ferromagnetic leads and the spin dependence of tunneling processes, the current flowing through such a diode becomes spin polarized and, interestingly, the spin polarization may change with reversing the bias voltage. In fact, very recently spin diode behavior was predicted and observed experimentally in another class of molecular structures, namely in single-wall carbon nanotubes [25, 26]. In this work we propose a *molecular* spin diode based on single molecule magnets. The considered system consists in particular of a SMM weakly coupled to one nonmagnetic and one ferromagnetic lead of high spin polarization; Fig. 1(b). To determine the transport properties of such a system we employ the real-time diagrammatic technique (RTDT), which allows us to systematically take into account the sequential and cotun-

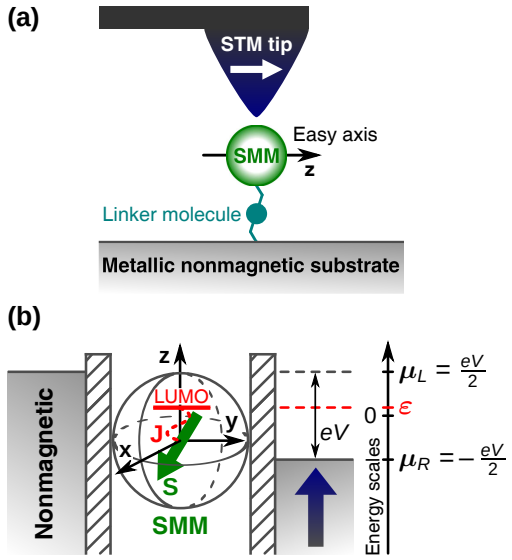

Fig. 1: (Color online) (a) Illustration showing a possible realization of a SMM-based device employing one metallic magnetic lead: the SMM molecule attached to a metallic *nonmagnetic* surface is pinned from the top by a *magnetic* STM tip. For simplicity, the magnetization of the tip and the molecule's easy axis are assumed here to be parallel. (b) Schematic of a SMM attached to one nonmagnetic (left) and one ferromagnetic (right) lead. The current flows due to tunneling through the LUMO level which is exchange coupled to the molecule's core spin S.

neling processes contributing to current. The sequential tunneling dominates the current for voltages larger than the Coulomb correlation energy and becomes exponentially suppressed in the Coulomb blockade regime, where transport is mainly due to cotunneling processes. As presented in the following, unequal couplings to the leads give rise to a pronounced asymmetry of spin-polarized current with respect to the bias reversal. Furthermore, in addition to the analysis of system's I-V transport characteristics, we also discuss the zero-frequency noise of tunneling current associated with discreteness of charge carriers (shot noise). The shot noise proves to be a source of useful information about various transport properties of the system, such as effective charges, coupling strengths or various types of correlations, which is hardly attainable from direct measurement of electric current [30].

Model and theoretical method. – We assume that transport through the molecule occurs only *via* the lowest unoccupied molecular orbital (LUMO) level, described by the energy ε and the local spin operator $\mathbf{s} = \frac{1}{2}\sum_{\sigma\sigma'} c_\sigma^\dagger \boldsymbol{\sigma}_{\sigma\sigma'} c_{\sigma'}$, which is coupled to the molecule's internal spin $\mathbf{S}$ *via* exchange interaction J. In principle, the exchange interaction can be either ferromagnetic or antiferromagnetic, depending on the specific type of a SMM. The molecule is thus fully characterized by Hamiltonian

$$\mathcal{H}_{\rm SMM} = -\Big[D + \sum_\sigma D_1\, c_\sigma^\dagger c_\sigma + D_2\, c_\uparrow^\dagger c_\uparrow c_\downarrow^\dagger c_\downarrow\Big] S_z^2 + \sum_\sigma \varepsilon\, c_\sigma^\dagger c_\sigma + U\, c_\uparrow^\dagger c_\uparrow c_\downarrow^\dagger c_\downarrow - J\mathbf{s}\cdot\mathbf{S}, \qquad (1)$$

where D is the uniaxial anisotropy constant of a neutral molecule, D_1 and D_2 stand for corrections to the anisotropy due to single and double occupation of the LUMO level, respectively, while U describes the Coulomb correlations between two electrons occupying the LUMO level. We note that although the corrections D_1 and D_2 to the anisotropy constant D are not crucial in observing the presented effects, we take them into account to make the model realistic. In Eq. (1) we neglected small transverse anisotropy [6]. Furthermore, it is assumed that the easy axis of the SMM is collinear with the magnetization of the right electrode, see Fig. 1(b), and both electrodes are described by noninteracting electrons, $\mathcal{H}_{\rm el} = \sum_q \sum_{\mathbf{k},\sigma} \varepsilon_{\mathbf{k}\sigma}^q\, a_{\mathbf{k}\sigma}^{q\dagger} a_{\mathbf{k}\sigma}^q$, with $\varepsilon_{\mathbf{k}\sigma}^q$ being the energy of an electron with the wave vector $\mathbf{k}$ and spin σ belonging to the lead q. Finally, the Hamiltonian describing tunneling processes between the molecule and the leads reads, $\mathcal{H}_{\rm T} = \sum_q \sum_{\mathbf{k},\sigma} \big[T_q\, a_{\mathbf{k}\sigma}^{q\dagger} c_\sigma + T_q^* c_\sigma^\dagger a_{\mathbf{k}\sigma}^q\big]$, where T_q denotes the tunnel matrix elements between the molecule and the qth lead. Coupling between the molecule and each lead can be expressed by $\Gamma_\sigma^q = 2\pi|T_q|^2\rho_\sigma^q$ and $\Gamma_q = (\Gamma_+^q + \Gamma_-^q)/2$. The spin polarization of the right magnetic lead is defined as $p = (\rho_+^R - \rho_-^R)/(\rho_+^R + \rho_-^R)$, where $\rho_{+(-)}^R$ is the density of states for the majority (minority) electrons.

To calculate the current flowing through the system we employ the real-time diagrammatic technique [27,28]. This approach allows us to take into account the first and second order tunneling processes through SMM in a fully systematic way [29]. Within the RTDT, the occupation probabilities P_χ of finding the system in a many-body state $|\chi\rangle$ are given by,

$$(\tilde{\mathbf{\Sigma}}\mathbf{P})_\chi = \Gamma\delta_{\chi\chi_0}, \qquad (2)$$

where $\tilde{\mathbf{\Sigma}}$ is the self-energy matrix accounting for various tunneling processes in the system, with a row χ_0 replaced by $(\Gamma,\ldots,\Gamma)$ due to normalization of probabilities. The current can be then calculated as

$$I = -\frac{ie}{2\hbar}\,{\rm Tr}\{\mathbf{\Sigma}^{\rm I}\mathbf{P}\}, \qquad (3)$$

with $\mathbf{\Sigma}^{\rm I}$ being the modified self-energy to take into account the number of electrons transferred through the system. Also the expression for the current noise in the limit of low frequencies [30],

$$S = 2\int_{-\infty}^{0} {\rm d}t\big[\langle I(t)I(0) + I(0)I(t)\rangle - 2\langle I\rangle^2\big] \qquad (4)$$

can be conveniently reformulated in the language of RTDT, for details see Ref. [31]. At this point, we ought to

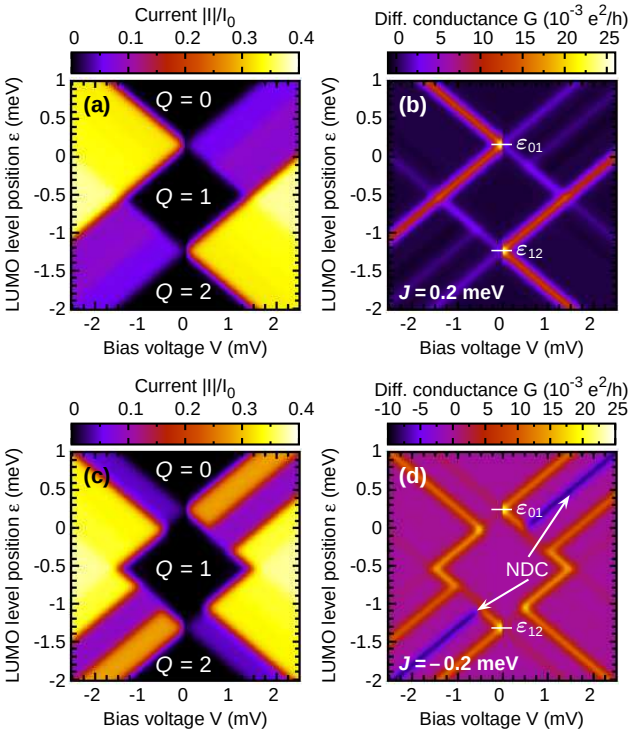

Fig. 2: (Color online) (a,c) The absolute value of the current I in units of $I_0 = 2e\Gamma/\hbar \approx 0.5$ nA, and (b,d) differential conductance G as a function of the bias voltage V and the LUMO level position ε for (a)-(b) *ferromagnetic* ($J > 0$) and (c)-(d) *antiferromagnetic* ($J < 0$) exchange coupling, $|J| = 0.2$ meV. Q in (a,c) represents the average charge accumulated in the LUMO level. The other parameters are: $S = 2$, $D = 50$ μeV, $D_1 = -5$ μeV, $D_2 = 2$ μeV, $U = 1$ meV, $k_BT = 40$ μeV, $p = 0.9$, and $\Gamma = \Gamma_L = \Gamma_R = 1$ μeV.

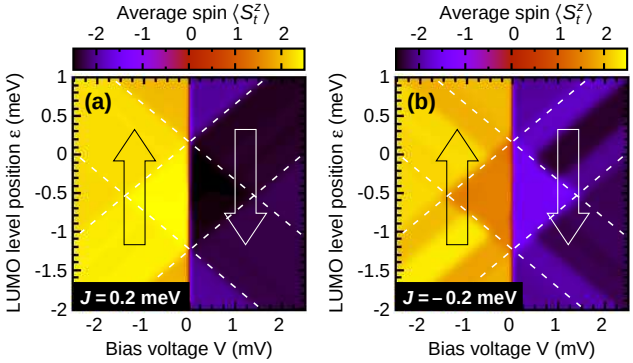

Fig. 3: (Color online) The zth component of the SMM's total spin $S_t^z = S_z + (c_\uparrow^\dagger c_\uparrow - c_\downarrow^\dagger c_\downarrow)/2$ as a function of the bias voltage V and the LUMO level position ε for (a) *ferromagnetic* and (b) *antiferromagnetic* exchange coupling. Hollow arrows depict the preferred direction of the SMM's spin with respect to the right lead's magnetic moment, whereas the dashed lines correspond to the position of main peaks in the differential conductance, Fig. 2(b,d) – i.e. they divide regions representing different occupation Q of the LUMO level. The remaining parameters are as in Fig. 2.

note that in the next section, rather than the shot noise S, we present the deviation of the current noise from its Poissonian value, described by the Fano factor $F = S/2e|I|$.

Finally, to determine the current order by order in tunneling processes, one performs perturbation expansion of the self-energies and probabilities in the coupling strength Γ [27, 28]. Here, we have taken into account the first and second order terms of expansion, which correspond to sequential and cotunneling processes, respectively [29, 32].

Results and discussion. – Since the model under consideration applies to various types of SMMs, here we present results only for the conceptually easiest case, though capturing essential physics, i.e. for a molecule with $S = 2$ and strong uniaxial magnetic anisotropy. Moreover, to keep the discussion most intuitive, we neglect the role of electron charge sign, assuming $e > 0$.

First of all, we note that due to large spin asymmetry in coupling of the SMM to the ferromagnetic lead, Fig. 1(b), the tunneling probability for spin-majority (spin-up) electrons is much larger than that for spin-minority (spin-down) electrons. On the other hand, the rate of tunneling processes between the molecule and the nonmagnetic lead is the same for both spin orientations. This generally leads to an asymmetry of tunneling current with respect to the bias reversal.

In Fig. 2(a)-(b) we display the current and differential conductance as a function of the LUMO level position and bias voltage for ferromagnetic ($J > 0$) interaction between the LUMO level and the SMM's spin. Close to the first resonance, $\varepsilon \approx \varepsilon_{01}$, see Fig. 2(b), current can flow easily from the ferromagnetic lead to the nonmagnetic one ($V < 0$), while it is suppressed for the opposite direction ($V > 0$); see also solid line in Fig. 4(a). To understand this behavior one should take into account the following facts. First, the molecule's states with one extra electron in the LUMO level correspond to the total spin number $S = 5/2$ and $S = 3/2$, with the former being of lower energy. Second, orientation of the molecule's spin depends significantly on the current direction, Fig. 3(a), and for $V > 0$ the SMM's spin tends towards antiparallel orientation with respect to the electrode's magnetic moment, whereas for $V < 0$ the spin prefers the parallel alignment. Thus, for low bias transport can occur mainly via the state corresponding to $S = 5/2$, and this requires spin-down electrons for $V > 0$ and spin-up electrons for $V < 0$. Unfortunately, tunneling rate for spin-down electrons is significantly reduced due to fewer available states in the minority spin band of the ferromagnetic lead, which effectively leads to the suppression of current for $V > 0$. When bias voltage increases, then the state corresponding to $S = 3/2$ becomes active in transport as well, leading only to a small increase of the current due to the spin selection rules for tunneling processes. However, the blockade for positive bias is removed when double occupancy of the LUMO level is admitted, which takes place for bias voltages exceeding some

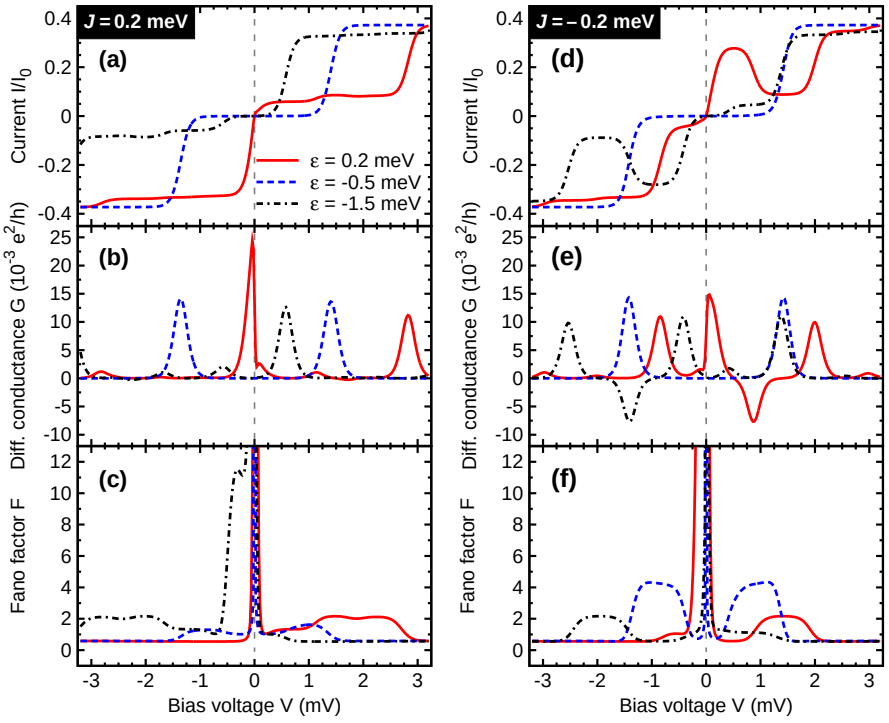

Fig. 4: (Color online) Selected cross-sections of density plots in Fig. 2 for specific values of the LUMO level position ε, which depict the current I flowing through the system (a,d), differential conductance G (b,e), and Fano factor F (c,f) as a function of the bias voltage V for the *ferromagnetic* (left panel) and *antiferromagnetic* (right panel) exchange couplings. The other parameters are the same as in Fig. 2. At low bias voltages the shot noise is dominated by thermal fluctuations while the current vanishes leading to a divergency in the Fano factor when $V \to 0$.

threshold value. Furthermore, the electron flow from ferromagnetic lead to the nonmagnetic one is spin polarized and degree of this polarization depends mainly on the spin polarization of the lead. In fact, in the case of a perfect halfmetallic ferromagnet ($p \to 1$), the current flowing towards halfmetallic lead would be totally blocked. Moreover, different time scales associated with spin-majority and spin-minority electrons lead in turn to considerable current fluctuations and super-Poissonian shot noise, see Fig. 4(c) for $\varepsilon = 0.2$ meV.

The situation becomes significantly different when the LUMO level is doubly occupied in equilibrium; $\varepsilon = -1.5$ meV in Fig. 4(a). Now, the behavior of current is reversed as compared to the case of $Q = 0$, since the current is suppressed for $V < 0$, i.e. for electrons tunneling from the magnetic lead. This is associated with the fact that an electron first has to tunnel out of the LUMO level and then another electron can enter the molecule. Thus, for positive bias a spin-up electron can easily tunnel out to the ferromagnetic lead. On the other hand, when the bias is reversed and the spin-down electron tunnels out of the molecule leaving it in the state corresponding to $S = 5/2$, the current becomes suppressed, as the rate for tunneling of spin-down electrons from the ferromagnetic lead to the molecule is relatively small. This also leads to super-Poissonian shot noise, as shown in Fig. 4(c).

More complex transport characteristics are observed when the exchange interaction is antiferromagnetic ($J < 0$); Fig. 2(c)-(d). The most striking difference is the appearance of additional peaks in the current when the LUMO level is initially either empty or doubly occupied, Figs. 2(c) and 4(d), which are accompanied by negative differential conductance (NDC); Figs. 2(d) and 4(e). Consider first the case of empty LUMO level in equilibrium, $\varepsilon = 0.2$ meV in Fig. 4(d). The key difference is that now the molecule's state corresponding to the total spin number $S = 3/2$ has lower energy and determines transport properties at low voltages. Thus spin-up electrons are involved in charge transport for $V > 0$ and spin-down electrons for $V < 0$. Consequently, the current is suppressed for negative bias and can easily flow for positive one. When the bias voltage reaches values admitting transport through the $S = 5/2$ state, the current for positive bias becomes suppressed by a spin-down electron tunneling to the LUMO level, while suppression for negative voltage becomes then lifted. In turn, when bias increases further admitting doubly occupation of the LUMO level, the blockade for positive bias becomes removed as well. Transport characteristics for doubly occupied LUMO level in equilibrium can be explained in a similar way.

On the other hand, when the LUMO level is singly occupied and its position corresponds approximately to the middle of the Coulomb blockade [dashed line in Figs. 4(a,d)], the diode behavior disappears and the cur-

rent recovers symmetry with respect to the bias reversal regardless of the type of the exchange interaction J. This is due to the fact that now with increasing the bias voltage all charge states of the molecule start taking part in transport at the same time, i.e. once the bias voltage reaches the threshold. The transport characteristics become then symmetric with respect to the bias reversal and the noise is rather sub-Poissonian, indicating the role of single-electron charging effects in transport. Note, however, that in the Coulomb blockade regime bunching of inelastic cotunneling processes may still result in enhancement of the shot noise; see dashed lines in Figs. 4(c,f). Furthermore, it is visible that in the case of $\varepsilon = -0.5$ meV the enhancement is much more pronounced in the case of the antiferromagnetic coupling, Fig. 4(f). Such a behavior stems from the fact that for $J < 0$ both energetically lowest lying molecular magnetic states $S_t^z = \pm 3/2$ allow the possibility of occupying the LUMO level by an electron either with the spin up or down, whereas for $J > 0$ the state $S_t^z = +5/2$ ($S_t^z = -5/2$) can only accommodate an electron with spin up (down). For this reason, in the former case both majority and minority electrons of the ferromagnetic lead can participate in transport, thus increasing the fluctuations.

To conclude, we have proposed a *molecular* spin diode based on single molecular magnets coupled to one ferromagnetic and one nonmagnetic leads. We have shown that the spin-dependent current flowing through the device becomes suppressed for one bias polarization and is enhanced for the opposite one. The suppressed transport is then accompanied with super-Poissonian shot noise. Moreover, we have demonstrated that the transport characteristics of SMM spin diodes strongly depend both on the number of electrons occupying the LUMO level, and on the type of exchange interaction between the LUMO level and the SMM's core spin. This gives the possibility to tune the functionality of a SMM spin diode by shifting the position of the LUMO level with a gate voltage.

Finally, we would like to note that although the presented results were calculated for a specific molecule with $S = 2$, the spin diode behavior can be observed in a large class of molecules. The main requirement is to have considerable spin asymmetry in the couplings to the left and right electrodes and well-defined spin states in the molecule, i.e. $J, D \gg T$, where T is the experimental temperature.

* * *

This work, as part of the European Science Foundation EUROCORES Programme SPINTRA, was supported by funds from the Ministry of Science and Higher Education as a research project in years 2006-2009 and the EC Sixth Framework Programme, under Contract N. ERAS-CT-2003-980409. The authors also acknowledge support from the Adam Mickiewicz University Foundation (M.M.), funds from the Ministry of Science and Higher Education as research projects in years 2008-2009 (M.M.) and 2008-2010 (I.W.), and the Foundation for Polish Science (I.W.).

REFERENCES

[1] Gatteschi D., Sessoli R. and Villain J., *Molecular Nanomagnets* (Oxford University Press, New York) 2006.
[2] Bogani L. and Wernsdorfer W., *Nature Mater.*, **7** (2008) 179.
[3] Mannini M., Pineider F., Sainctavit P., Danieli C., Otero E., Sciancalepore C., Talarico A.M., Arrio M.A., Cornia A., Gatteschi D. and Sessoli R., *Nature Mater.*, **8** (2009) 194.
[4] Timm C. and Elste F., *Phys. Rev. B*, **73** (2006) 235304.
[5] Misiorny M. and Barnaś J., *Phys. Rev. B*, **75** (2007) 134425.
[6] Misiorny M. and Barnaś J., *Phys. Stat. Sol. B*, **246** (2009) 695.
[7] Lu H.-Z., Zhou B. and Shen S.-Q., *Phys. Rev. B*, **79** (2009) 174419.
[8] Barraza-Lopez S., Park K., García-Suárez V. and Ferrer J., *J. Appl. Phys.*, **105** (2009) 07E309.
[9] Barraza-Lopez S., Park K., García-Suárez V. and Ferrer J., *Phys. Rev. Lett.*, **102** (2009) 246801.
[10] Heersche H. B., de Groot Z., Folk J. A., van der Zant H. S. J., Romeike C., Wegewijs M. R., Zobbi L., Barreca D., Tondello E. and Cornia, A., *Phys. Rev. Lett.*, **96** (2006) 206801.
[11] Ni C., Shah, S., Hendrickson D. and Bandaru, P. R., *Appl. Phys. Lett.*, **89** (2006) 212104.
[12] Jo M.-H., Grose J. E., Baheti K., Deshmukh M. M., Sokol J. J., Rumberger E. M., Hendrickson D. N., Long J. R., Park H. and Ralph, D. C., *Nano Lett.*, **6** (2006) 2014.
[13] Henderson J. J., Ramsey C. M., del Barco E., Mishra A., and Christou, G., *J. Appl. Phys.*, **101** (2007) 09E102.
[14] Voss S., Zander O., Fonin M., Rüdiger U., Burgert M. and Groth, U., *Phys. Rev. B*, **78** (2008) 155403.
[15] Fonin M., Voss S., Herr S., de Loubens G., Kent A.D., Burgert M., Groth U., and Rüdiger U., *Polyhedron*, **28** (2009) 1977.
[16] Zobbi L., Mannini M., Pacchioni M., Chastanet G., Bonacchi D., Zanardi C., Biagi R., Pennino U.D., Gatteschi D., Cornia A., and Sessoli R., *Chem. Commun.*, **12** (2005) 1640.
[17] Abdi A.N., Bucher J.P., Rabu P., Toulemonde O., Drillon M., and Gerbier P., *J. Appl. Phys.*, **95** (2004) 7345.
[18] Cornia A., Costantino A.F., Zobbi L., Caneschi A., Gatteschi D., Mannini M., and Sessoli R., *Struct. Bond.*, **122** (2005) 133.
[19] Naitabdi A., Bucher J.P., Gerbier P., Rabu P., and Drillon M., *Adv. Mater.*, **17** (2005) 1612.
[20] Burgert M., Voss S., Herr S., Fonin M., Groth U., and Rüdiger U., *J. Am. Chem. Soc.*, **129** (2007) 14362.
[21] Rudziński W. and Barnaś J., *Phys. Rev. B*, **64** (2001) 085318.
[22] Wilczyński M., Świrkowicz R., Rudziński W., Barnaś J. and Dugaev V., *J. Magn. Magn. Mater.*, **290** (2005) 209.

[23] Souza F. M., Egues J. C. and Jauho A. P., *Phys. Rev. B*, **75** (2007) 165303.
[24] Hamaya K., Kitabatake M., Shibata K., Jung M., Ishida S., Taniyama T., Hirakawa K., Y. A. and Machida T., *Phys. Rev. Lett.*, **102** (2009) 236806.
[25] Merchant C. A. and Marković N., *Phys. Rev. Lett.*, **100** (2008) 156601.
[26] Weymann I. and Barnaś J., *Appl. Phys. Lett.*, **92** (2008) 103127.
[27] Schoeller H. and Schön G., *Phys. Rev. B*, **50** (1994) 18436.
[28] König J., Schmid J., Schoeller H. and Schön G., *Phys. Rev. B*, **54** (1996) 16820.
[29] Misiorny M., Weymann I. and Barnaś J., *Phys. Rev. B*, **79** (2009) 224420.
[30] Blanter Y. and Büttiker M., *Phys. Rep.*, **336** (2000) 1.
[31] Thielmann A., Hettler M., König J. and Schön G., *Phys. Rev. B*, **68** (2003) 115105.
[32] Weymann I., *Phys. Rev. B*, **78** (2008) 045310.

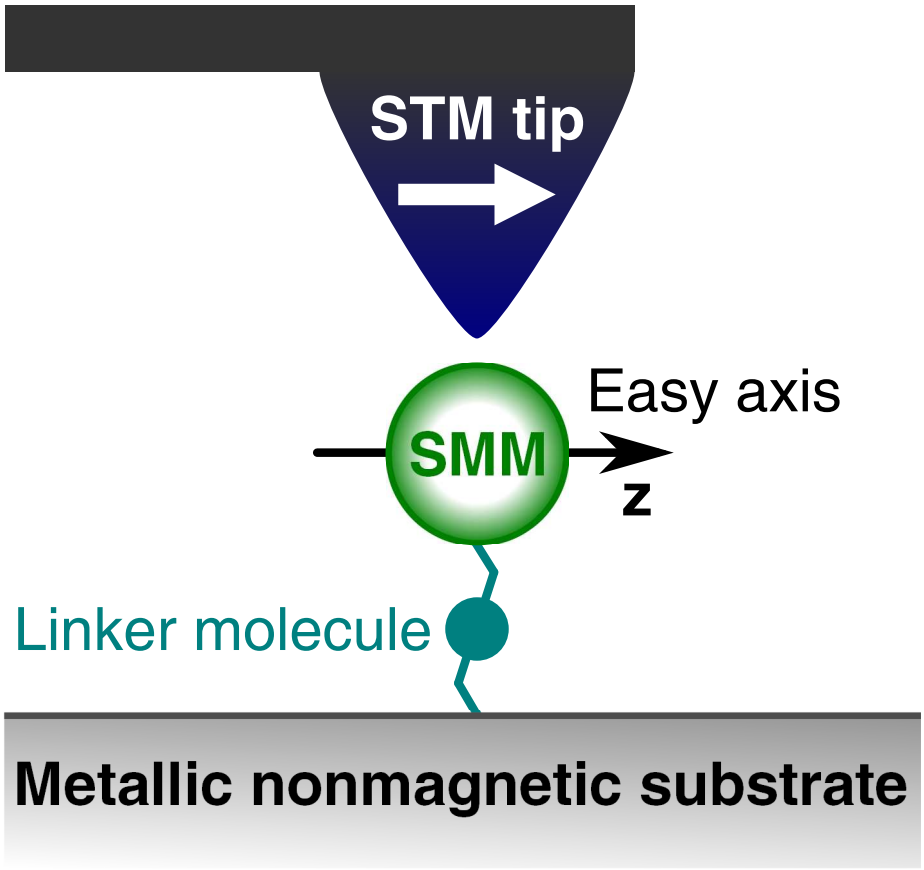
STM tip
Easy axis
SMM
z
Linker molecule
Metallic nonmagnetic substrate